Politecnico di Torino, Master's Degree in Electrical Engineering, March 2023

STUDY AND ADVANCED MODELLING OF MULTIPHASE MOTORS WITH RECONFIGURABLE NUMBER OF PHASES

Supervisors
Prof. Gianmario PELLEGRINO
Dr. Simone FERRARI

ETEL SA Tutor
Dr. Alessandro FASOLO

Candidate
Lorenzo CIFALINO'

***Abstract*—This thesis focuses on Permanent Magnet Synchronous Motors with multi-threephase configurations. The use of multi-phase solutions enables improvements in efficiency, cost optimization and and integrated system utilization, in line with the latest market trends. These improvements are made possible by the integration of new technologies, such as SiC and GaN-based devices. The aim of this work is to upgrade a three-phase ETEL motor by modifying the winding and control strategy into twelve-phases without modifying its active parts. The electromagnetic study has been executed through FEM analysis using FEMM as client of Matlab within the open-source environment SyR-e. The control strategy has been tested in a Simulink ambient using a common-differential mode control written in C-language. The six-phase and twelve-phase configurations have been explored and compared with the threephase motor, proving what was expected.**

I. Multi-threephase motors modelling

A. Winding configuration

The initial three-phase machine with concentrated, double layer windings has been reconfigured as asymmetric quadruple three-phase, with a phase distance of $\gamma = 180°/N_{ph} = 15°$ from one three-phase set to another. Fig.1 shows the space axis of the twelve-phases and an example of waveforms, with the currents phase $90°_{el}$ ahead of the open-circuit flux linkages.

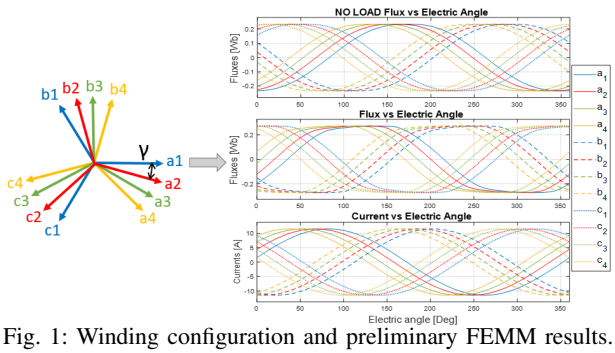

Fig. 1: Winding configuration and preliminary FEMM results.

B. Motor Model: Vector Space Decomposition (VSD)

Each current-star is linked to an own Clarke transformation, as in equation (1), with a phase angle $(N-1)\cdot\gamma$ (with N = 1,..4) with respect to the reference three-phase system N = 1.

$$[C_N] = \frac{2}{N_{ph}} \cdot \begin{bmatrix} cos(\gamma_{s_N}) & cos(\gamma_{s_N} + \frac{2\pi}{3}) & cos(\gamma_{s_N} + \frac{4\pi}{3}) \\ sin(\gamma_{s_N}) & sin(\gamma_{s_N} + \frac{2\pi}{3}) & sin(\gamma_{s_N} + \frac{4\pi}{3}) \\ 1/2 & 1/2 & 1/2 \end{bmatrix} \quad (1)$$

Furthermore, the *VSD* modelling technique has been used to represent the multi-phase machine dynamics, using the "T_{12}" transformation to describe the twelvephase system in the (α, β) sub-plane for the energy conversion and utilizing the others (x_k, y_k) to represent higher order harmonics and unbalances. Finally, the zero-sequence is neglected since the three-phase stars are isolated. The resulting equations system is in (2) for a twelvephase machine.

$$\begin{aligned} [v_{\alpha,\beta}] &= [R_s]\cdot[i_{\alpha,\beta}] + \frac{d[\lambda_{\alpha,\beta}]}{dt} \\ [v_{x_k,y_k}] &= [R_s]\cdot[i_{x_k,y_k}] + \frac{d[\lambda_{x_k y_k}]}{dt} \quad k = 1,2,3 \\ [v_{o_N}] &= [R_s]\cdot[i_{o_N}] + \frac{d[\lambda_{o_N}]}{dt} \quad N = 1,2,3,4 \end{aligned} \quad (2)$$

C. Motor Control

The adopted common and differential mode control is explained in Fig.2, where with the common-mode components command energy conversion by averaging across sets, while the differential-mode is controlled to zero to avoid unbalance. The reference torque corresponds to a certain current value using MTPA trajectory as a LUTs. Besides, each common and differential mode has an own PI-controller. A decoupling matrix [D] was adopted, considering the differences between systems 1-2, 2-3, 3-4. In Fig.3 the general flux-observer scheme is evidenced. As regards the duty-cycles computation, the third harmonic is injected and the dead-time has been compensated. In addiction, a phase-advancing strategy has been chosen to avoid the implementation delay.

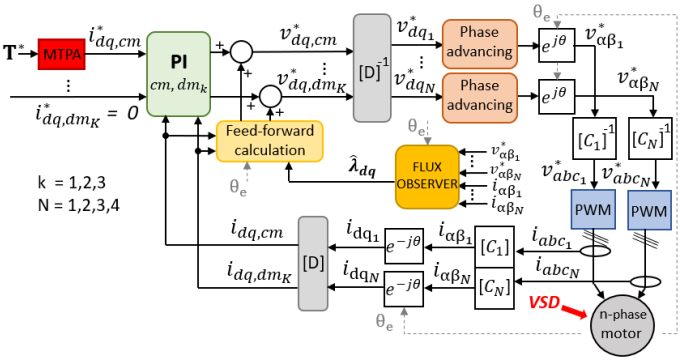

Fig. 2: Common ad differential mode control scheme.

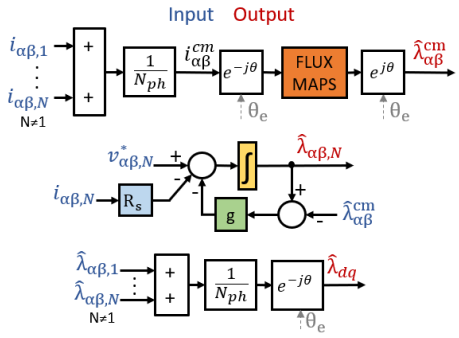

Fig. 3: General N-3-phase flux-observer scheme.

II. Results

The ETEL original torque-motor considered in this work is the *TMK0291-050-3VBS*. Its main data are in Table I.

TABLE I: Main data of **TMK0291-050-3VBS** threephase motor.

Motor Performance	Unit	Value
Continuous torque T_c	Nm	271
Continuous current I_c	A	32.5
Electrical resistance R_s @20°C	Ω	0.66
Electrical inductances L_d/L_q	mH	6.5/5.05
Max speed with flux-weakening ω_{max}	rpm	2410
Rated speed ω_0	rpm	387
Number of poles	-	44
Rated DC bus voltage V_{DC}	V	600
External diameter	cm	310
Length	cm	50

A. FEM Analysis

The tool-chain used to achieve the goal is depicted in Fig.4. The maps have been generated using an I_{dq} grid, with a maximum value of three times the nominal current considered. The contributions of iron losses, eddy-current losses, and magnet losses have been calculated analytically using Steinmetz equations, as FEMM cannot perform time-harmonic simulations. Finally, the quantities obtained have been utilized in post-processing analysis and control simulations.
Table II points out the improvements provided by the multiphase motors for both versions studied.

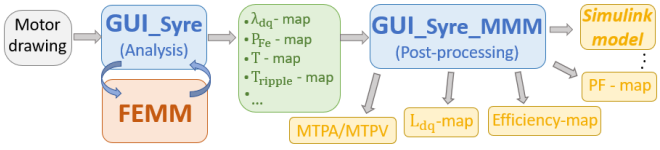

Fig. 4: Simulation chain adopted for the analysis.

TABLE II: Sixphase and twelvephase motors' quantities comparison respect to the threephase one.

Quantities	6-phase	12-phase
Ripple peak to peak of nominal torque	−86%	−91.4%
Average nominal torque	+2.7%	+4.2%
Iron losses @Rated working-point	−2%	−6%
Efficiency speed range @87%	+7%	+14%
Efficiency @Rated working-point	+1.7%	+2%
Iron losses speed range @200W-Low load	+80%	+100%
Power factor @Rated working-point	+2.2%	+2.3%
DC Bus-voltage V_{DC}	=	=
L_d inductance	+28%	+173%
L_q inductance	+36%	+172%

B. Simulink Model

As can be noticed in Fig.4, the Simulink model can be achieved as part of the post-processing analysis,enabling the control strategy used to be verified. Digital sampling phenomena were taken into account for the power electronics, as well as for PWM signal generation through the use of a comparison between a carrier signal and a triangular waveform.
Moreover, the same microprocessor model was used to control different independent inverter structures.
The motor model used the VSD technique, and flux-current relations were modeled with pre-obtained LUTs. The same approach was taken for the computation of iron losses.
In simulation an high dynamic could be tested, verifying the correctness of the code with a dragged load, as shown in Fig.5.

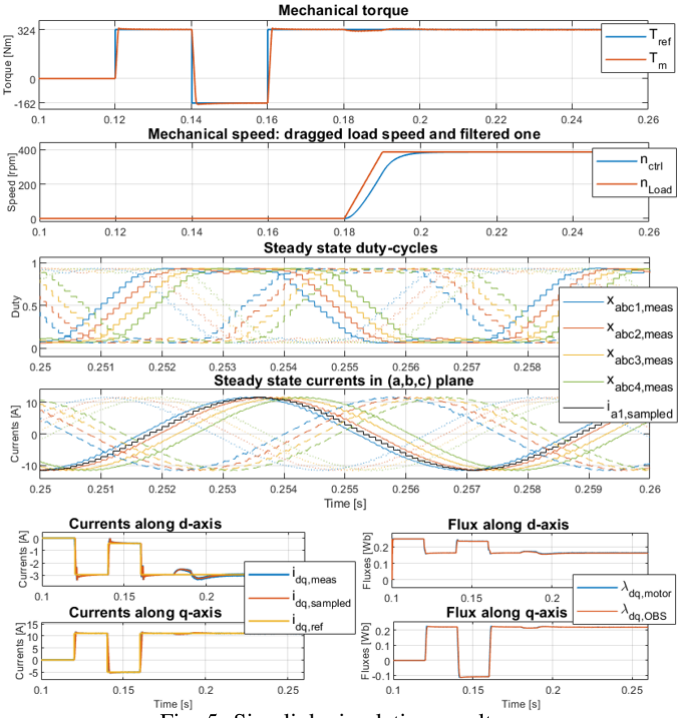

Fig. 5: Simulink simulation results.

III. Conclusion

The benefits of reconfiguring a 44-poles three-phase PMSM into a twelve-phase one are shown in terms of torque quality, efficiency, and extended speed range. These advantages are due to the improved flux linkage deriving from each winding, now affected by only one or two magnetic poles and not by four as in the three-phase motor, with a consequent considerable reduction of harmonic phenomena. The latter allows to reach a better thermal behaviour of the machine. Additionally, the increased value of inductance reduces the PWM current ripple and the related torque ripple and iron loss.
Ultimately,the new solutions can be considered part of an integrated system that could optimize space, volume, and cost in a future product, making it an attractive option for customers.